Case Study

Seismic Response Case Study of Isolated Floor System Having Special Biaxial Spring Units

Shenlei Cui[1]; Michel Bruneau, F.ASCE[2]; and Amarnath Kasalanati, P.E.[3]

Abstract: This paper presents the results of a shake-table case study conducted on a proposed novel type of isolated floor system having special bidirectional spring units. This solution provides enhanced seismic performance for certain facilities where constraints may require isolation of select floors or spaces rather than the entire structure (typically for selected rooms in critical facilities). This system was tested on a 6-DOF shake table. The floor seismic excitations were obtained from nonlinear time history analyses of both single-degree-of-freedom and multidegree-of-freedom frames stiffened with buckling restrained braces and designed as a structural fuse frame, and subjected to synthetic ground motions. The test results show that the isolated floor system performs satisfactorily, but that system behavior differs from that of the spring units alone because correction must be made to account for sources of friction beyond those from the spring units alone. The mechanical properties of the isolated floor system are also obtained in terms of the acceleration–displacement relationship, which provides the foundation to better simulate these isolated floor systems in future parametric studies. **DOI: 10.1061/(ASCE)ST.1943-541X.0001596.**

Author keywords: Isolation; Isolated floor; Seismic; Performance; Floor acceleration; Displacement response; Earthquake engineering; Structural fuse; Seismic effects.

Introduction

There has been a growing interest worldwide to protect critical nonstructural components, when isolating the entire structure is not possible or practical. Several systems have been developed that use gravity or springs for recentering and friction or viscous dampers to provide damping (e.g., Kemeny and Szidarovszky 1995; Kasalanati et al. 1997; Arima et al. 1997; Kaneko et al. 1995; Wang et al. 2014; Shi et al. 2014). The system discussed in this paper employs a unique bidirectional spring (Cui et al. 2010) to provide stiffness, damping, and recentering capabilities. This system is different from other spring-based systems because a single bidirectional spring is active in any horizontal direction as opposed to the need for using orthogonal springs in other systems. This allows the system to be compact, and it can be used for isolating a single item (server cabinet, artwork) or an entire floor (a computer access floor). Modeling of the bidirectional spring was described in detail by Cui et al. (2010). This paper presents the results of research conducted as a continuation of that work, wherein the individual spring units are used here in a whole system with realistic surrounding conditions.

Knowledge of the nonlinear behavior of the bidirectional springs alone is not sufficient to understand and/or predict system behavior because experience has shown that some behaviors are often observed at the system level under seismic excitation. Therefore, focus in this paper is on characterization of behavior and mechanical properties (such as force-displacement or acceleration–displacement relationships) of the complete isolated floor system that could be used to simulate its dynamic response in various applications using available computer programs. Although findings from this study provide new knowledge and quantifications that could not have been otherwise assessed, the work here is referred to as a case study because it focuses on a single floor geometry. In the characterization tests, to simulate the realistic conditions to be encountered when a floor isolation system is installed in an existing room, a surrounding masonry wall was built and some steel edge plates were used to cover the space between the isolated floor system and the wall. Two sets of 2,627 N/m nominal stiffness spring units were investigated for this isolated floor system. Both synthetic ground motions and the analytical floor response of both single-degree-of-freedom (SDOF) and multidegree-of-freedom (MDOF) structural fuse frames were used as seismic inputs. Besides unidirectional tests, some bidirectional tests were also conducted. Different load cases, both with symmetric and eccentric configurations of gravity loads, were considered. The mechanical properties of this system are presented in terms of the acceleration-displacement relationship. Test results are compared from different points of view, including comparison of behavior between the multidirectional spring units and the corresponding complete isolated floor system.

Note that whereas various equipment isolation systems have been developed focusing on the response of single equipment (Demetriades et al. 1992; Lambrou and Constantinou 1994; Kemeny and Szidarovszky 1995; Kasalanati et al. 1997; Fathali and Filiatrault 2007, to name a few); here the interest is on isolated floor systems for applications to protect nonstructural components that can be moved and located anywhere on the floor of specific rooms (as often required in critical facilities, such as hospitals and emergency management centers, or as a substitute to raised computer floors). A few complete floor isolation systems have been developed and implemented in Japan (Arima et al. 1997), either using

[1]Engineering Specialist, INTECSEA WorleyParsons Group, Houston, TX 77079. E-mail: shenlei.cui@gmail.com

[2]Professor, Dept. of Civil, Structural and Environmental Engineering, Univ. at Buffalo, State Univ. of New York, Buffalo, NY 14260 (corresponding author). E-mail: bruneau@buffalo.edu

[3]Director, Dept. of Engineering, Dynamic Isolation Systems, Inc., Sparks, NV 89434. E-mail: akasalanati@dis-inc.com

Note. This manuscript was submitted on March 6, 2015; approved on May 1, 2016; published online on July 11, 2016. Discussion period open until December 11, 2016; separate discussions must be submitted for individual papers. This paper is part of the ***Journal of Structural Engineering***, © ASCE, ISSN 0733-9445.

gravity based systems (using suspension mechanisms) or linear spring based systems (coil springs or rubber units used for restoration force) coupled with viscous dampers or lead plugs used for damping. Kaneko et al. (1995) report that a floor isolated system in the Kansai area worked effectively during the 1995 Hyogoken-Nanbu Earthquake. The system proposed here is novel in that it uses a relatively simple and low-cost special kind of bidirectional spring units to provide stiffness, damping, and selfcentering capabilities to the isolated floor.

Isolated Floor System Description

The isolated floor system considered here (shown in Fig. 1) has two main components. First, a raised steel floor frame on casters having a wheel diameter of approximately 152 mm (6 in.) and bolted to the steel floor frame vertically to support the gravity loads. Second, two sets of bidirectional spring units used to decouple the response of the isolated floor (and of the nonstructural components it supports) from the motion of the building floor itself. Each biaxial spring unit [shown in Fig. 2(a)], bolted to the building floor, essentially consist of a helicoidal spring enclosed inside an HSS tube, as conceptually illustrated in Fig. 2(b). A steel cable connects the spring inside the HSS to the isolated floor. That cable passes through a bushing that serves to provide smooth curvature from a horizontal spring to the vertical contact with the isolated floor, while accommodating 180° rotation of the cable in the vertical plane and 360° rotation in the horizontal plane. The cable is finally connected to a second bushing itself tied to the underside of the isolated floor. The geometric details of the bushings and the damping provided by the sliding of the cable on those bushings is beyond the scope of this paper; it is presented in Cui et al. (2010, 2012), along with physical models able to replicate the hysteretic behavior of the spring alone [shown in Fig. 2(c)]. The hysteresis loop of the bidirectional spring has four distinct segments: a steep initial segment up to 76 mm (3 in.), followed by a relatively flat secondary stiffness branch, a flat returning stiffness and slightly steeper return to zero in the last 76 mm (3 in.). The geometry to the bidirectional spring is the reason for this hysteresis loop, which is explained in greater detail in Cui et al. (2010). The rising rate of the restoring force with respect to displacement significantly drops down to the system's second stiffness at displacement larger than approximately 76 mm (3 in.).

Floor panels (i.e., tiles) with a steel surface are bolted down to the floor frame and provide the walking surface (using panels allows easy access, if needed, the bidirectional spring units after the system has been set up). The total height of this isolated floor system is approximately 324 mm (12.75 in.). Note that floor height of this system in the field have ranged from 178 mm (7 in.) to 1,219 mm (48 in.). The total weight of this isolated floor is approximately 8,522 N (1,916 lb).

Note that the approach taken in this experimental research focused on investigating fundamental behavior as opposed to validating a specific design procedure. As such, because of isolated floors having set properties (i.e., two different spring stiffnesses) were subjected to a number of different gravity load conditions and different seismic excitations, such as to obtain a broad range of responses that cover the wide range of isolation floor periods that are typically used in the field.

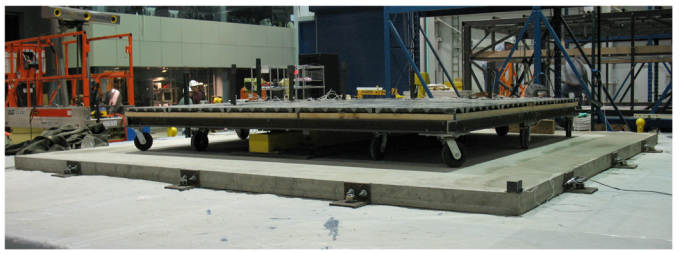

Fig. 1. Overview of isolated floor system (without wall and steel edge plates)

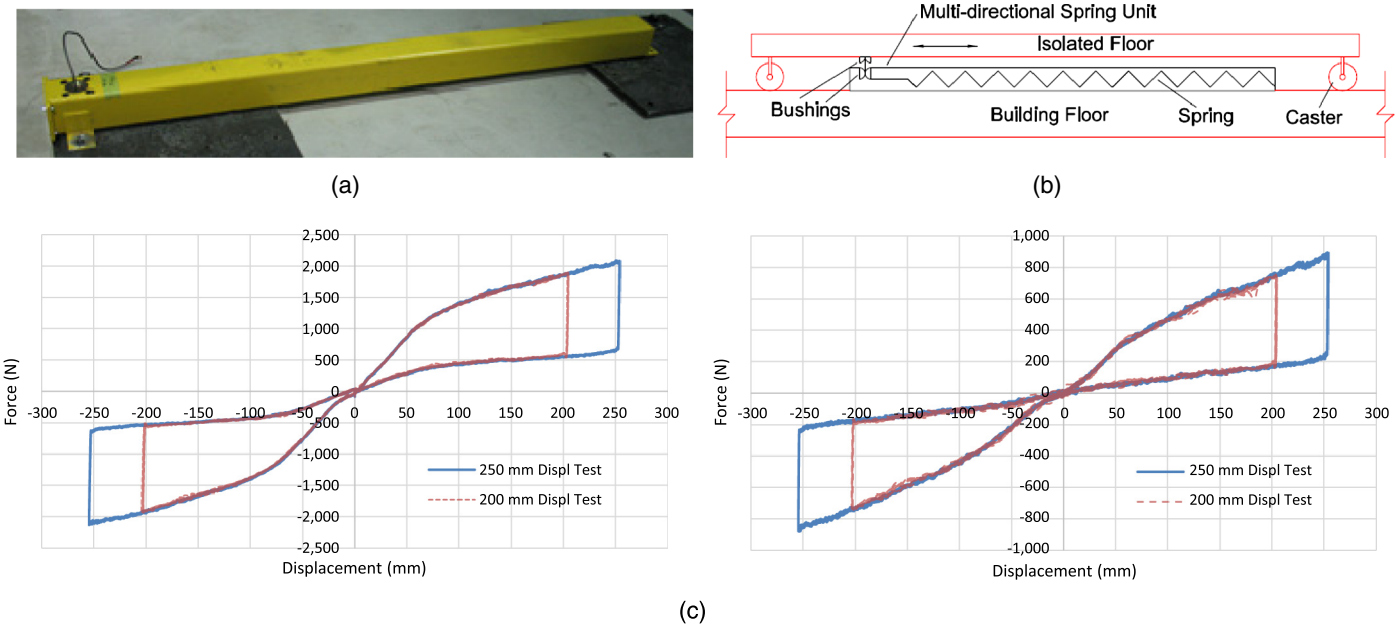

Fig. 2. Biaxial spring unit: (a) overview; (b) application in isolated floor system; (c) hysteretic behavior of 2,627 and 1,313 N/m spring units (data from Cui et al. 2012)

Test Setup

Specimen Assembly and Setup

A 102 mm (4 in.) thick concrete slab was designed and cast to simulate the structural floor surface on which isolated floors would be installed in a typical application. The surface of this concrete slab was finished by hand to a smoothness similar to concrete floor surfaces in buildings. No special finish was applied on the surface of this concrete slab. Furthermore, to simulate the constraints of installing such an isolated floor system in building rooms, a 610 mm (24 in.) tall masonry wall was built on the concrete slab, as shown in Fig. 3. Note that the space equivalent to a door opening was also included in the wall. The inside area bounded by the wall was $3{,}454 \times 3{,}454$ mm (136×136 in.), which corresponds to the size of a small room. The concrete slab was fixed onto the shake table platform by steel angles (L4 × 6) and anchors bolted on the four sides of the footing slab. Note that some threaded rods were precast into the slab at the corresponding positions of the anchors.

Two bidirectional spring units with a nominal stiffness of 2,627 N/m (15 lb/in.) were bolted down to steel plates which were themselves connected to the shake table by bolts running through holes in the concrete footing slab, as shown in Fig. 3(a). Two floor modules were assembled together above the multidirectional spring units to create the complete isolated floor system surface, as shown in Fig. 3(b). During their installation, the cables of the two spring units underneath were pulled out 51 mm (2 in.) and attached to the steel floor frame such as to pretension the springs before the tests. As explained in Cui et al. (2010), this pretension improves the initial rigidity of the system and its recentering capability after an event. Finally, eight (8) steel edge plates, each 1,727 mm (half of the inner length of each side of the surrounding wall, 68 in.) long, 610 mm (24 in.) wide, and 4.8 mm (3/16 in.) thick, were directly screwed down to the top surface of the 2×6 in. wood boards which were fixed onto the surrounding masonry wall. The bottom surface of the edge plates and the walking surface of the isolated floor were at the same level. These steel edge plates were used to cover the space between the isolated floor and the surrounding concrete masonry wall. One end of each edge plate was cut at an angle to form symmetric edges at the wall corners, as shown in Fig. 3(c). The resulting isolated floor system specimen is shown in Fig. 3(d).

Load Program

Two load criteria were used for the gravity load design of the isolated floor system: a concentrated load and a uniformly distributed load. First, the floor was designed to a stress of 0.012 MPa (250 psf) over the footprint of the point load applied to the floor system. Second, the floor was designed to carry a uniformly distributed load of 50 psf over its entire area.

Cases with concentric and eccentric distribution of gravity load were considered for the tests of the isolated floor system. Steel

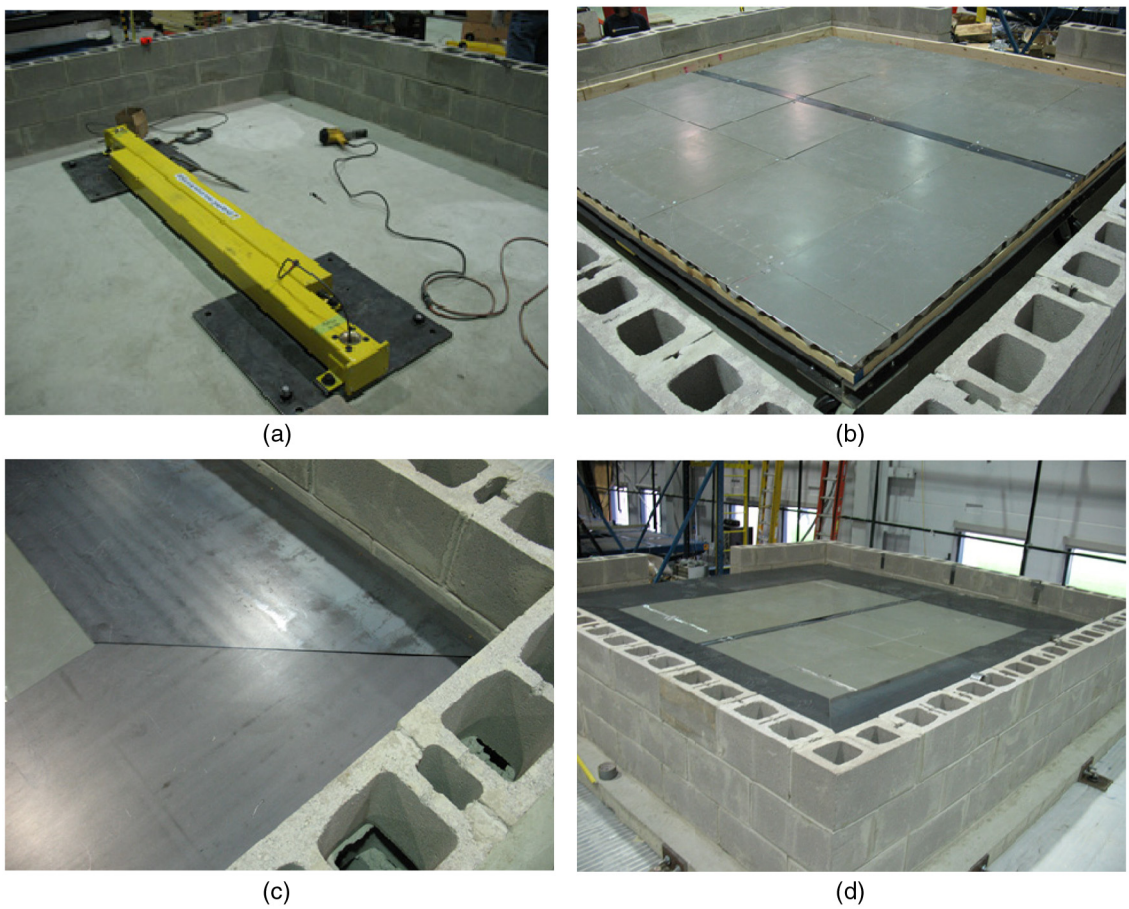

Fig. 3. Overview of isolated floor system specimen: (a) fixture of spring units; (b) assembly of two modules of the isolated floor system; (c) corner configuration of edge plates in isolated floor system; (d) overall view of the system (lighter grey surface is the movable isolated floor; darker grey is the set of edge plates attached to the concrete wall)

Table 1. Summary of Load Cases

Load case number	Applied load [Pa (psf)]	X direction eccentricity (%)	Y direction eccentricity (%)
1	0 (0)	0	0
2	1,200 (25)	0	0
3	2,304 (48)	0	0
4	647 (14)	0	0
5	1,194 (25)	12	0
6	647 (14)	12	12
7	1,194 (25)	19	0
8	647 (14)	19	19
9	Cabinet	—	—
10	Cabinet	—	—

Note: Uniformly distributed load value is calculated based on the area enclosed by the surrounding wall; eccentricity percentage is calculated as eccentricity divided by the inner dimension bounded by walls; for load cases 9 and 10, the applied load is referred to as *Cabinet*. Explanation is provided in the text.

plates, ranging from 620 to 6,700 N, and lead bricks, each weighing 111 N, were placed at various locations on the isolated floor to create different load cases. Ten different load cases in total were used to test this isolated floor system under various conditions, which are summarized in Table 1. Load Cases 1 to 3 investigate the behavior of this isolated floor system under different symmetric load cases, with uniformly distributed gravity loads of 0, 25, and 48 psf over the entire area of the isolated floor system. Also, to compare the behavior of this isolated floor system under concentric and eccentric loads and between different magnitudes of eccentricity, tests with Load Cases 5 to 8 were conducted. Load Cases 5 and 7 corresponded to the floor subjected to the same gravity load magnitude as Load Case 2, but with two different values of eccentricity with respect to the x direction. For Load Cases 6 and 8, although the intent was to create a load magnitude as in Load Case 2, when attempting to locate the steel plates to create the eccentricities needed in the x and y directions, it was found that the local load value calculated based on the footprint of the steel plate on the floor exceeded the maximum permitted for the floor walking surface. Because creating large eccentricities had priority over maintaining the load magnitude, Load Cases 6 and 8, therefore, ended up being designed with a load magnitude of 14 psf instead of 25 psf, but with the correct desired eccentricities. To be able to compare the behavior of the system with the symmetric layout of masses and eccentric layout of masses, Load Case 4 was created with a load magnitude of 14 psf, which is the same as Load Cases 6 and 8, but with symmetric load layout.

Note that in all cases, although the uniformly distributed loads were calculated and reported as if applied over the entire floor area, the steel plates could only be applied to the part of the isolated floor system that would not touch the edge plates during earthquake motions. More details about the load application and load cases are provided in Cui et al. (2012).

Load Cases 9 and 10 were intended to simulate the consequence on behavior of heavy furniture placed on the edge cover plates against the design intent, such as a heavy file cabinet sitting both on the steel edge plate and on the isolated floor. For Load Case 9, a small cabinet $381 \times 673 \times 737$ mm ($15 \times 26.5 \times 29$ in.) in size was filled with 27 lead bricks, with a total weight of 3,002 N (675 lb), and placed as shown in Fig. 4. Load Case 10 was similar, but with the same file cabinet located entirely on the edge cover plate instead of partly resting on it. Fig. 4 shows Load Cases 1, 2, 5, 6, 9, and 10.

Input Program

The characterization tests of the isolated floor system included both unidirectional and bidirectional tests. For the unidirectional tests, a spectra compatible acceleration time history was generated using the Target Acceleration Response Spectra Compatible Time Histories (*TARSCTHS*) Code for a building located in Sherman Oaks, California, with site soil-type class B. The design spectral accelerations for this site are $S_{DS} = 1.3$ g, and $S_{D1} = 0.58$ g for 2% probability of exceedance in 50 years. This ground motion (Acc01) was used to either test the isolated floor system directly (i.e., at ground level), or as input in analyses to generate floor response time histories. Absolute floor acceleration response obtained from structural fuse frames models analyzed using *SAP2000* were used as seismic inputs to test the isolated floor system. Note that in a structural fuse concept, passive energy dissipation (PED) devices are designed such that all seismically induced damage is concentrated on the PED devices, allowing the primary structure to remain elastic during seismic events (Vargas and Bruneau 2006a, b; Cui et al. 2012). The structures designed under this concept are stiff, leading to a decrease in drift demands on the nonstructural components, but acceleration demands can be significantly larger.

One of the floor motions used (Acc11) corresponds to a single-degree-of-freedom (SODF) structural fuse frame with a natural vibration period of 0.53 s, another (Acc31) to the third story response of a four-story, three-bay structural fuse frame; both frames, which used buckling resistant braces (BRBs) as energy dissipation devices in each story, were designed by Vargas and Bruneau (2006a). Another time history considered (Acc002) was obtained from the actual structural fuse frame specimen tested by Vargas and Bruneau (2006b). In this specific test, the shake table input motion was a synthetic ground motion generated to match the design response spectrum (based on the National Earthquake Hazard Reduction Program Recommended Provisions (NEHRP 2003) for Sherman Oaks, California, and site soil-type class B, and scaled to 0.75 g (the shake table testing program included ground motions scaled to multiple peak-ground acceleration levels).

Some bidirectional tests were also conducted. One set of combined bidirectional inputs (denoted as C1) considered Acc01 and Acc02 as inputs in the E-W and N-S directions, respectively (being synthetic ground motions for the same Sherman Oaks location mentioned above), whereas a second set (denoted C2) considered Acc11 and Acc31 in the E-W and N-S directions, respectively. Note that to investigate response of the isolation floors subjected to bi-directional excitations, for sake of investigating behavior, combining ground motions from various sources was deemed an expedient method to provide uncorrelated ground motions to reflect the fact that the period of a building is not necessarily the same in both directions.

These seismic inputs were gradually scaled up to different amplitudes to make the isolated floor system reach a displacement response of approximately 127 mm (5 in.) in unidirectional tests and 102 mm (4 in.) in bidirectional tests unless such displacements could not be reached because of the limits in the displacement capacity of 152 mm (6 in.) of the shake table in Structural Engineering and Earthquake Simulation Laboratory at the University at Buffalo.

Response spectra of four input motions (Acc01, Acc02, Acc11, and Acc31) are presented in Fig. 5. As seen from this figure, these input motions had strong acceleration content in the 0- to 1-s period range, which excites nonstructural components. Details of all acceleration records considered are presented in Cui et al. (2012).

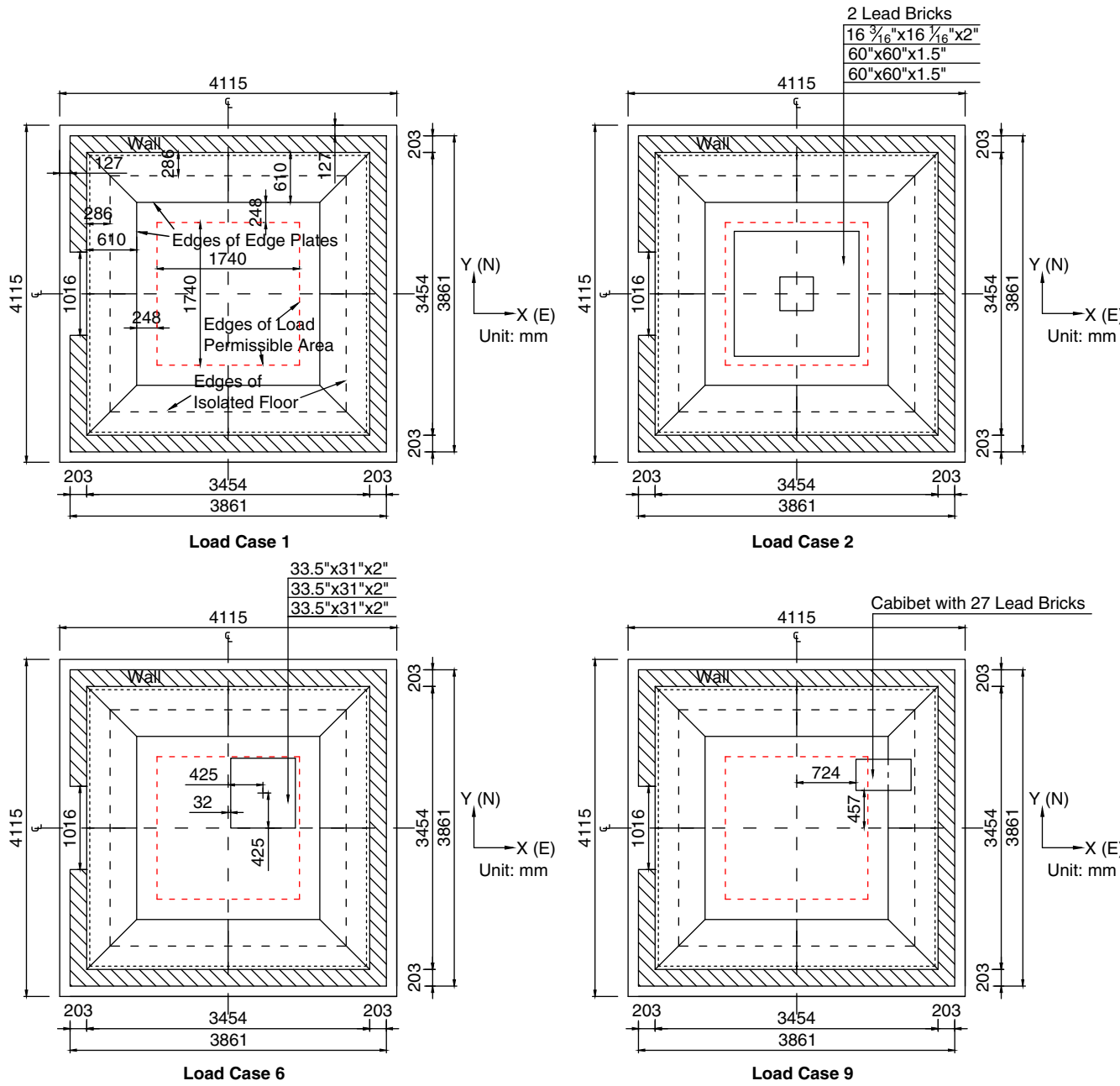

Fig. 4. Top view of selected load cases

Instrumentation

The objective of these characterization tests was to capture the force-displacement behavior of the isolated floor system and compare the resulting performance with that of the nonisolated floor. Here, *force* indicates the restoring force of the isolated floor system, and *displacement* is the relative displacement of the isolated floor with respect to the base. The restoring force of this system was calculated from the acceleration response of the isolated floor. Displacement and acceleration response of both the shake table and the isolated floor were measured. Furthermore, to instigate the rotation motion of the isolated floor, it was decided to measure the displacement response at both ends of each side of the isolated floor. Twenty-four instrumentation channels in total were used to record the response of the specimen, namely, twelve accelerometers and twelve *string pots* displacement transducers. Details are provided in Cui et al. (2012).

Test Protocol

Four unidirectional input motions (Acc002, Acc01, Acc11 and Acc31) and two bidirectional input motions (C1 and C2) were applied on various load cases of the isolated floor. The test program is presented in Table 2, where the nomenclature of the test name is constructed by sequentially referring to load case number first, and the input motion name second. For example, *1Acc002* indicates the test of the floor under Load Case 1 when subjected to input Acc002. Also, the letters *wo* have been added at the end of the name for the tests conducted on the isolation system without edge plates. Those tests were conducted to compare the behavior of the isolated floor system between cases with and without edge plates and

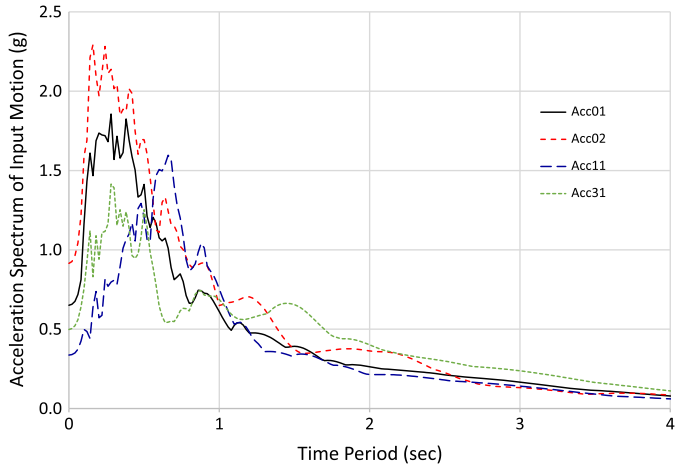

Fig. 5. Comparison of response spectra of different input motions used in testing

Table 2. Test Sequences of Isolated Floor System

Test number	Test name	Input name	Load case number	Edge plates
1	1Acc002	Acc002	1	With
2	1Acc01	Acc01	1	With
3	1Acc11	Acc11	1	With
4	1Acc31	Acc31	1	With
5	1C1	C1	1	With
6	1C2	C2	1	With
7	2Acc002	Acc002	2	With
8	2Acc01	Acc01	2	With
9	2Acc11	Acc11	2	With
10	2Acc31	Acc31	2	With
11	2C1	C1	2	With
12	2C2	C2	2	With
13	3Acc11	Acc11	3	With
14	3Acc31	Acc31	3	With
15	3C2	C2	3	With
16	4C2	C2	4	With
17	5C2	C2	5	With
18	6C2	C2	6	With
19	7Acc002	Acc002	7	With
20	7Acc01	Acc01	7	With
21	7Acc11	Acc11	7	With
22	7Acc31	Acc31	7	With
23	7C2	C2	7	With
24	8Acc31	Acc31	8	With
25	8C1	C1	8	With
26	8C2	C2	8	With
27	9Acc31	Acc31	9	With
28	9C2	C2	9	With
29	10Acc31	Acc31	10	With
30	10C1	C1	10	With
31	10C2	C2	10	With
32	2Acc31wo	Acc31	2	Without
33	2C2wo	C2	2	Without
34	3Acc31wo	Acc31	3	Without
35	3C2wo	C2	3	Without

without the surrounding concrete masonry wall. Note that tests without the surrounding wall allowed the researchers to investigate the performance of the spring units as part of the isolated floor system when subjected to larger displacements. Moreover, this edge condition is typical in cases where the isolation system is used as a stand-alone platform rather than as an isolated floor.

Test Results

General

Shake table test results are summarized in Table 3. The response quantities included are: the peak displacement of the shake table (PTD), the peak displacement of the isolated floor (PFD), the peak acceleration of the shake table (PTA), the peak acceleration of the isolated floor (PFA), the maximum rotation angle of the isolated floor, and the peak relative displacement of the isolated floor with respect to the shake table. The small differences in the maximum rotation angles obtained in the E-W and N-S directions are because the large displacement theory was not used to correct the data (Cui et al. 2012). However, the rotation angle is small in all cases, and not significant enough to warrant further precision. Isolation was effective for load cases 1 through 8 and representative response spectral reductions for test 3C2 are presented in Fig. 6. Isolated platform provided effective reduction of acceleration content in the 0- to 1-s period range. As seen from this figure, there is slight amplification in the isolated platform response beyond the 2-s period. This is attributable to higher response closer to the isolated period and the presence of friction in the system that prevents effective isolation at low accelerations at a long period. It is noted that the frequency of most of the sensitive components supported by the base isolated floor are in the 1- to 30-Hz frequency range and therefore a slightly higher response beyond the 2-s period (below 0.5 Hz) is not considered detrimental.

Selected typical results of the tests for isolated floor systems using spring units having a nominal stiffness of 2,627 N/m (15 lb./in.) are presented in Figs. 7–12. The rest of the test results in Table 3 are presented in Cui et al. (2012). Each of Figs. 7–12 contains four plots. Plots (a) and (b) respectively illustrate the displacement and acceleration of both the shake table and the isolated floor as a function of time, for comparison purpose. The third plot (c) illustrates the rotation of the isolated floor as a function of time. The relative displacement of the isolated floor can be inferred from the difference between the two curves in part (a) of each figure. A time history plot of that relative displacement by itself is not provided here, but relative displacements are presented from a more significant perspective in the fourth plot (d) of each figure, which describes the mechanical behavior of the isolated floor system in terms of absolute acceleration versus the relative displacement of the isolated floor with respect to the shake table (because the restoring force of the isolated floor system is a function of this displacement). Even though it is understood that acceleration and displacement are typically out of phase, here, the sign of acceleration has been reversed to make the curve resemble the restoring force-displacement relationship of the system. For consistency, this was also done in the plots of the acceleration time histories of the system [i.e., part (b) of each figure].

Concentric Load Case Results

Throughout all these characterization tests, no damage occurred to the isolated floor system itself. Fig. 7 shows the typical response of the isolated floor system (with edge plates) for a unidirectional earthquake floor excitation. Note from Fig. 7(a) that the floor displacement response generally follows the shake table excitation, but the relative displacement between the isolated floor and the shake table is significant enough to produce the isolation effect. Also, note from Fig. 7(c) that the rotation of the system is not significant, which is less than 0.014 rad (i.e., 0.8°). It can also be observed from the part (c) of other figures that the rotation angle of the isolated floor is not significant. Figs. 8 and 9 present the response

Table 3. Summary of Peak Values of Response Quantities for Isolated Floor System Having 2,627 N/m Multidirectional Spring Units

Test number	Test name	Peak table absolute displacement (mm)		Peak floor absolute displacement (mm)		Peak table absolute acceleration (g)		Peak floor absolute acceleration (g)		Maximum rotation (10^{-3} rad)		Peak relative displacement (mm)	
		E-W	N-S	E-W	N-S	E-W	N-S	E-W	N-S	E-W	N-S	E-W	N-S
1	1Acc002	47.1	—	71.2	—	1.24	—	0.29	—	4.7	4.3	57.8	—
2	1Acc01	152.2	—	160.4	—	0.74	—	0.31	—	2.8	4.7	66.0	—
3	1Acc11	151.3	—	187.4	—	0.40	—	0.43	—	4.2	4.9	124.0	—
4	1Acc31	152.4	—	206.9	—	0.46	—	0.39	—	4.0	4.9	77.4	—
5	1C1	153.1	152.5	203.9	226.8	0.76	0.98	0.33	0.40	8.4	10.9	76.6	98.8
6	1C2	155.7	155.1	260.7	225.5	0.40	0.45	0.38	0.39	14.9	13.9	128.5	146.0
7	2Acc002	46.3	—	60.1	—	1.20	—	0.15	—	9.8	7.5	72.5	—
8	2Acc01	125.3	—	144.8	—	0.60	—	0.18	—	6.0	6.5	64.4	—
9	2Acc11	156.5	—	215.4	—	0.42	—	0.19	—	8.4	8.1	153.7	—
10	2Acc31	153.4	—	185.3	—	0.46	—	0.18	—	9.7	11.6	130.5	—
11	2C1	151.4	151.9	223.7	214.3	0.75	0.97	0.16	0.20	19.3	20.0	177.6	189.9
12	2C2	155.1	155.0	238.5	196.2	0.41	0.46	0.19	0.17	12.6	13.8	210.2	132.1
13	3Acc11	143.1	—	197.4	—	0.30	—	0.14	—	11.4	10.5	169.0	—
14	3Acc31	208.7	—	256.4	—	0.50	—	0.15	—	10.7	11.6	239.5	—
15	3C2	117.4	116.7	180.8	154.8	0.34	0.34	0.14	0.14	18.4	18.8	198.0	152.5
16	4C2	154.7	155.7	222.1	204.7	0.41	0.46	0.25	0.21	14.8	15.5	146.4	148.1
17	5C2	152.1	155.5	238.2	206.0	0.40	0.45	0.30	0.24	50.3	50.8	219.7	142.4
18	6C2	152.5	152.0	223.0	200.1	0.41	0.45	0.25	0.21	36.5	36.5	155.7	149.5
19	7Acc01	149.7	—	200.8	—	0.75	—	0.20	—	25.5	27.4	119.1	—
20	7Acc11	154.8	—	194.7	—	0.41	—	0.20	—	38.5	42.2	152.2	—
21	7Acc31	156.5	—	172.8	—	0.46	—	0.19	—	21.5	21.8	107.0	—
22	7C2	152.7	156.8	214.5	209.7	0.41	0.45	0.21	0.18	68.0	71.2	191.5	156.3
23	8Acc31	156.7	—	188.1	—	0.47	—	0.22	—	19.3	20.6	92.0	—
24	8C1	150.1	153.3	206.2	227.1	0.76	1.01	0.22	0.23	56.6	63.6	132.6	180.8
25	8C2	154.0	157.7	209.1	204.5	0.42	0.45	0.25	0.22	39.5	41.2	155.4	132.0
26	9Acc31	156.9	—	159.1	—	0.47	—	0.29	—	15.2	34.8	30.0	—
27	9C2	152.8	157.3	154.6	178.6	0.41	0.45	0.38	0.27	22.6	24.3	86.9	70.7
28	10Acc31	156.7	—	165.0	—	0.47	—	0.28	—	10.4	12.2	55.9	—
29	10C1	150.6	153.6	176.1	200.6	0.77	1.02	0.33	0.37	24.7	28.4	70.0	76.6
30	10C2	152.9	156.6	213.8	187.4	0.41	0.45	0.41	0.28	25.1	25.0	117.6	97.5
31	2Acc31wo	152.7	—	218.6	—	0.44	—	0.19	—	12.2	30.7	150.7	—
32	2C2wo	157.5	154.5	253.2	196.3	0.40	0.44	0.19	0.17	19.2	35.1	235.8	162.1
33	3Acc31wo	152.0	—	222.1	—	0.43	—	0.14	—	17.4	18.6	185.8	—
34	3C2wo	118.9	115.3	192.2	149.6	0.29	0.33	0.13	0.12	26.5	28.8	191.8	121.6

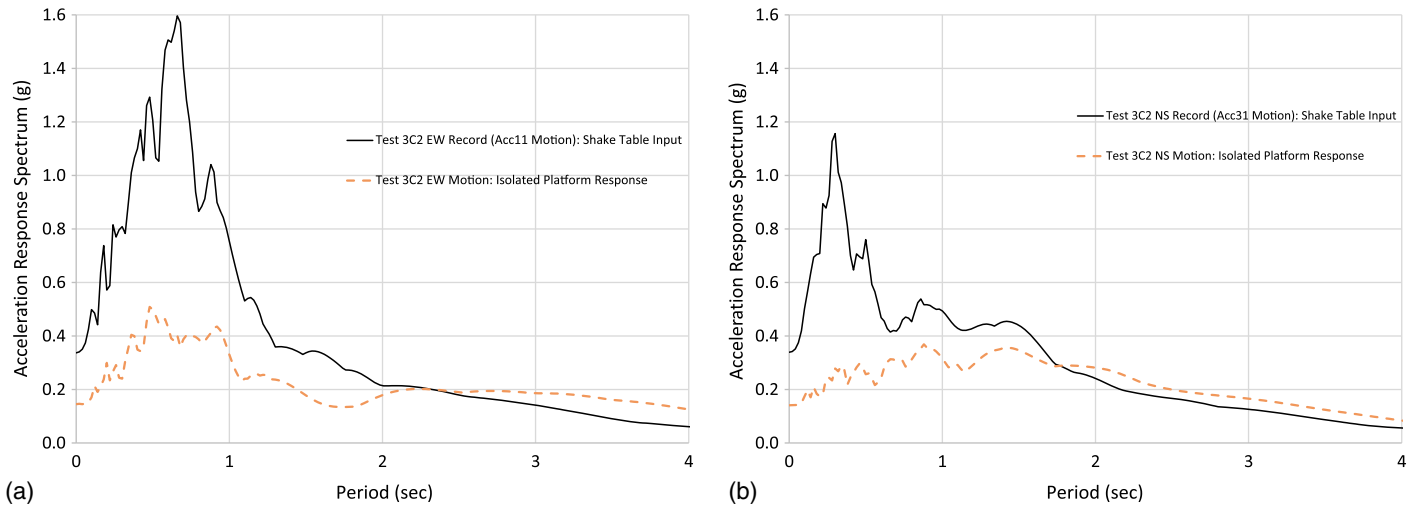

Fig. 6. Comparison of response spectra of shake table input motion and isolated floor response for bidirectional test 3C2 in: (a) EW direction; (b) NS direction

for a bidirectional earthquake input. Again, the displacement response of the isolated floor and the shake table excitation are generally in phase as observed before. Furthermore, there is a general similarity in the acceleration-displacement plot (d) between the unidirectional test 2Acc11 (Fig. 7) and the E-W component of the bidirectional test 2C2 (Fig. 8). The acceleration-displacement hysteretic curve for the N-S component of the bidirectional test 2C2 (Fig. 9) is slightly more erratic. This may be attributable to the fact

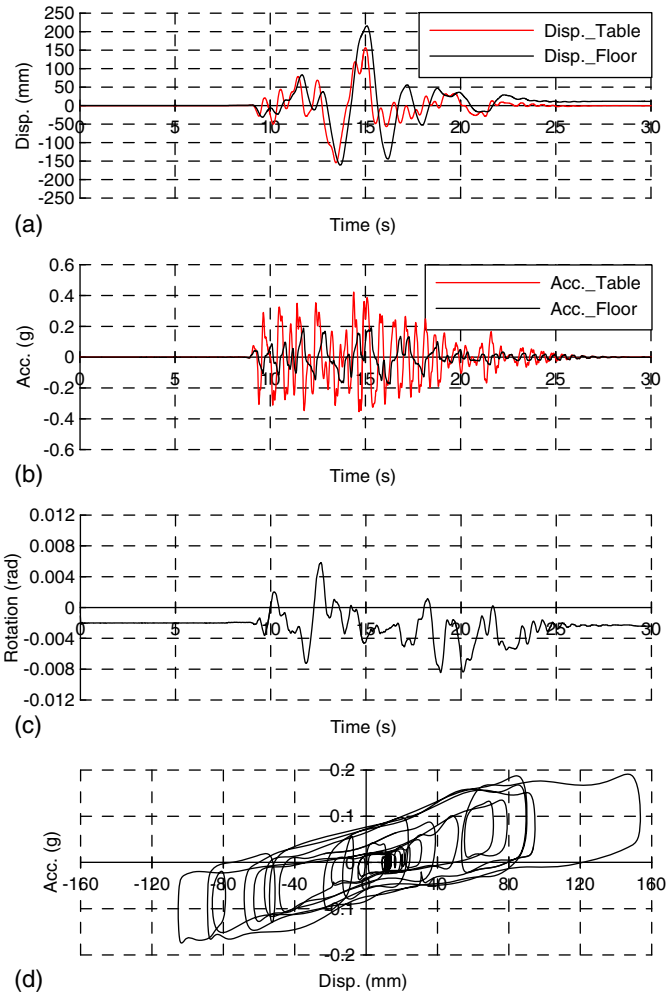

Fig. 7. Results of test 2Acc11: (a and b) displacement and acceleration of shake table and isolated floor, respectively; (c) rotation; (d) acceleration-displacement relationship of isolated floor system

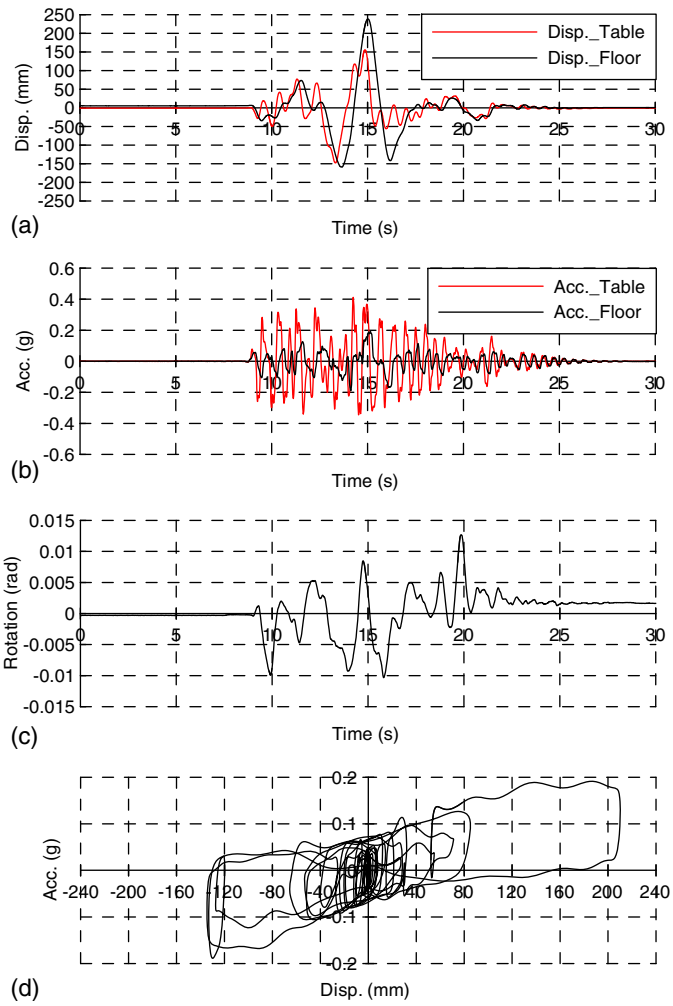

Fig. 8. Results of test 2C2 in E-W direction: (a and b) displacement and acceleration of shake table and isolated floor, respectively; (c) rotation; (d) acceleration-displacement relationship of isolated floor system

that the cable of the spring unit circles around the brass bushing surface in a horizontal plane during bidirectional motion.

Edge Loading with Impeded Motion

Figs. 10 and 11 show the typical results for Load Cases 9 and 10, respectively. Note that during the tests under Load Cases 9 and 10, where a small file cabinet filled with lead bricks was located on top of and/or across the edge plates, the isolated floor only moved slightly relatively with respect to the shake table. This is logical because it is much harder for the isolated floor to be effective for these two load cases. The file cabinet impeded the movement of the floor by creating significant friction between the walking surface and the cabinet in Load Case 9 and between the walking surface and the steel cover plates in Load Case 10. Because the cabinet was not positioned symmetrically, this restraint was more effective on the side of the isolated floor where the cabinet was located, resulting in a more noticeable floor rotation—even though the magnitude of these rotations remained modest. The cabinet did vibrate and slide a little during the tests. However, it did not overturn or hit against the wall.

Peak Displacement and Acceleration Responses

In Table 3, note that the peak displacement response of the isolated floor is larger than the corresponding displacement of the shake table. The peak acceleration response of the isolated floor is reduced compared with the corresponding input acceleration of the shake table. Two notable exceptions to this behavior are Load Case 1 (with no imposed load on the isolated floor) and Load Case 9 (with a cabinet on the floor and edge plate). Lack of adequate mass was the reason for Load Case 1 to have a reduced isolation effect. For Load Case 9, the cabinet spanning the floor and edge plate impeded the free movement of the floor and negatively affected the isolation effectiveness.

As shown in the typical Figs. 7(d)–12(d), the acceleration-displacement relationship of the isolated floor system exhibits hysteresis. The friction between the cable and the brass bushing of the spring units contributes to this hysteresis. Furthermore, the loops for unidirectional tests agree with each other well, which indicates the behavior of the isolated floor system is stable under repeated motions. For the two 2,627 N/m (15 lb/in.) nominal stiffness multidirectional spring units used in the isolated floor system under a given isolated weight of 8,522 N (1,916 lb) (i.e., Load Case 1), the slope of the system second stiffness is $(27\ \text{lb/in.} \times 2)/(1{,}916\ \text{lb/g}) = 0.028\ \text{g/in.}$ (where g = acceleration of gravity), which is equivalent to a maximum acceleration plateau. Therefore, the acceleration-displacement relationship of the isolated floor system is almost flat at displacements larger than 76 mm (3 in.) as shown in each part (d) of Figs. 7–12 (for cases with or without edge

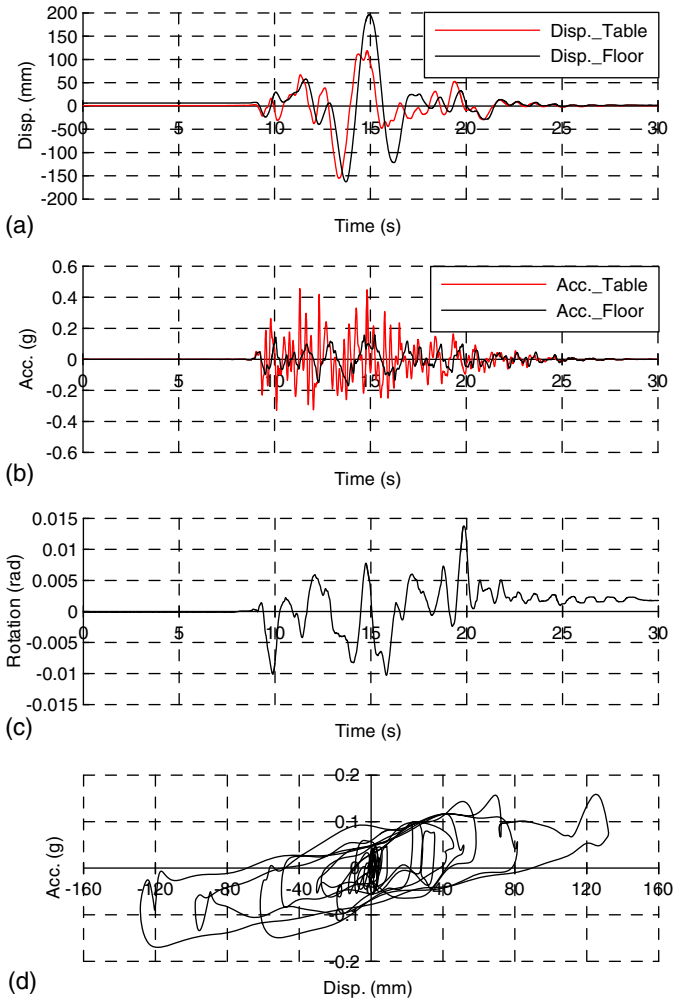

Fig. 9. Results of test 2C2 in N-S direction: (a and b) displacement and acceleration of shake table and isolated floor, respectively; (c) rotation; (d) acceleration-displacement relationship of isolated floor system

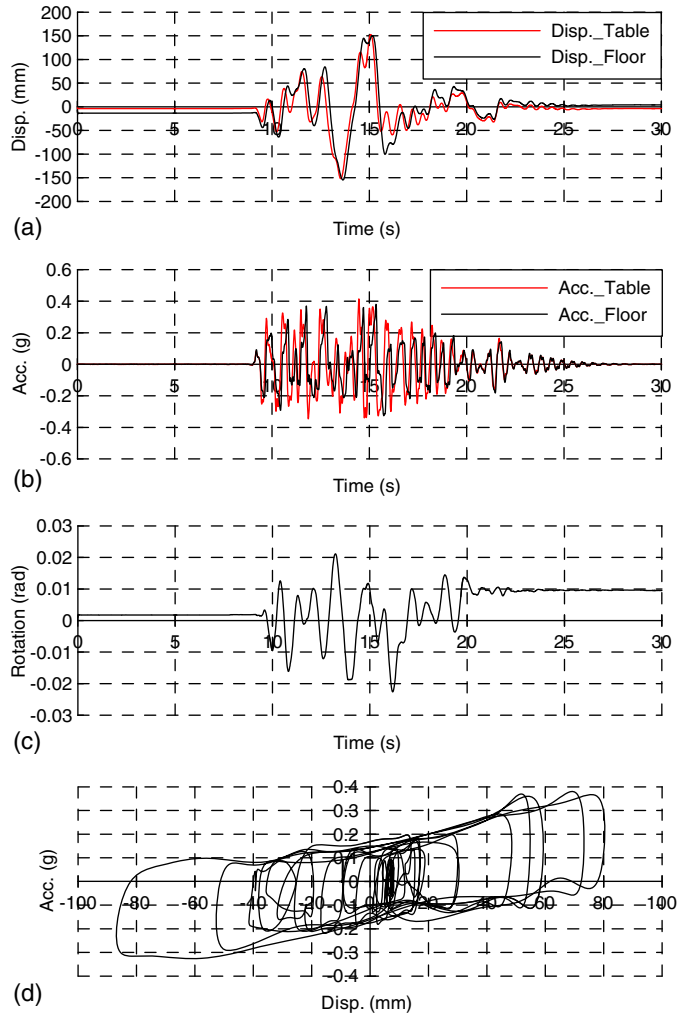

Fig. 10. Results of Test 9C2 in E-W direction, with movement impeded with the cabinet: (a and b) displacement and acceleration of shake table and isolated floor; (c) rotation; (d) acceleration-displacement relationship of isolated floor system

plates). Furthermore, when the isolated mass becomes larger, the maximum acceleration response of the isolated floor system decreases because the second stiffness of the given spring units is a constant value and is divided by larger isolated mass. In other words, with larger imposed loads, the isolated period of the system is larger and the isolation effect is greater.

Unidirectional versus Bidirectional Tests

From the data in Table 3, it may be observed that the peak acceleration response of the isolated floor in bidirectional tests is almost the same as in unidirectional tests for each load case (i.e., for a given value of gravity load and load configuration). For example, the peak acceleration response of the isolated floor in tests of 3Acc11, 3Acc31, and 3C2 is 0.14 g, 0.15 g in unidirectional cases, and 0.14 g in both directions, respectively. This is an expected result because at relatively large displacement [larger than approximately 76 mm (3 in.)] the slope of the system second stiffness in the acceleration-displacement is a maximum acceleration plateau, and the displacements in the above cases were significantly more than 76 mm. Also, it is observed that the peak relative displacement of the isolated floor in both directions (198.0 and 152.5 mm, respectively) of 3C2 are different from the corresponding values in the corresponding unidirectional tests (169.0 mm in 3Acc11 and 239.5 mm in 3Acc31, respectively). This is because the second stiffness slope is entered when the resultant spring elongation exceeds 76 mm, which occurs at smaller displacements in each component direction.

Variation over Multiple Tests

To investigate whether the behavior of the isolated floor system is stable when subjected to different unidirectional seismic inputs, the comparison of the acceleration-displacement relationships for the symmetric load cases (Load Cases 2 and 3) is plotted in Figs. 13 and 14, respectively. It is observed that the acceleration-displacement loops, under the same load case, when subjected to different seismic inputs agree well with each other, confirming the behavior of this isolated floor system is stable when subjected to different seismic excitations.

Variation for Different Gravity Loads

To investigate how the behavior of the isolated floor system (with edge plates on) changes under unidirectional seismic inputs and different applied gravity loads, the test results for Load Cases 1

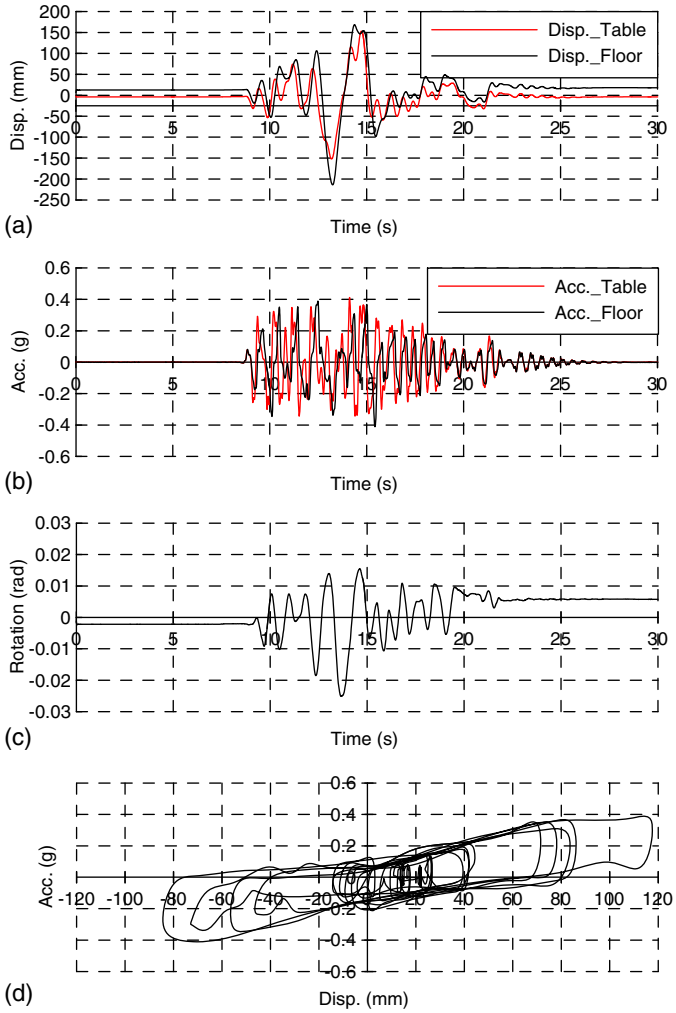

Fig. 11. Results of Test 10C2 in E-W direction, with motion partially impeded: (a and b) displacement and acceleration of shake table and isolated floor; (c) rotation; (d) acceleration-displacement relationship of isolated floor system

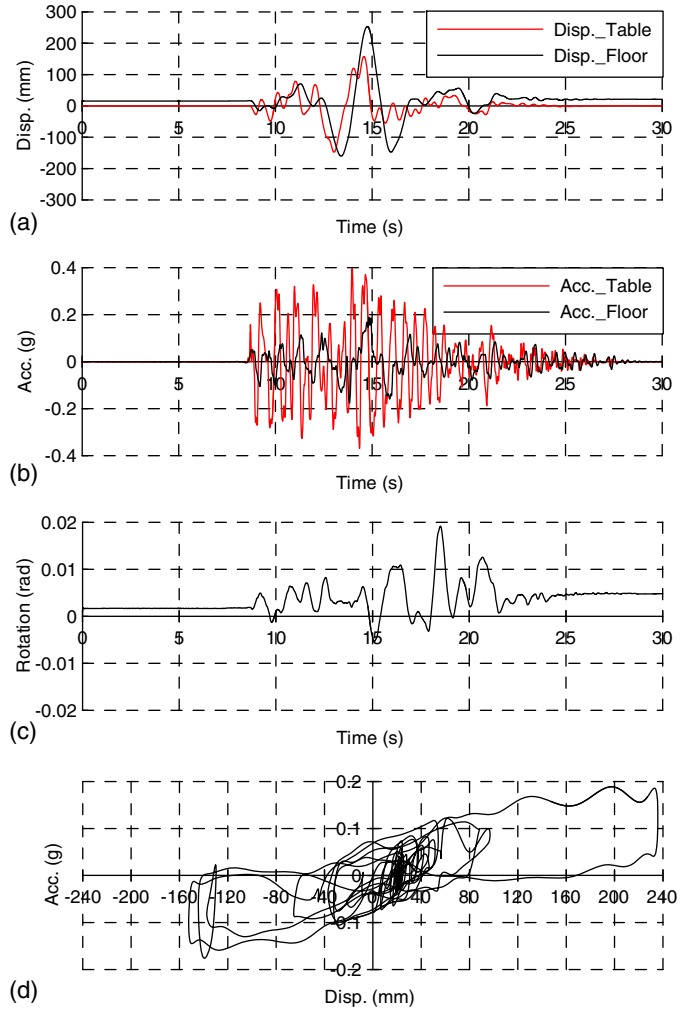

Fig. 12. Results of Test 2C2wo in E-W direction: (a and b) displacement and acceleration of shake table and isolated floor, respectively; (c) rotation; (d) acceleration-displacement relationship of isolated floor system

to 3 under shake table excitation inputs Acc11 and Acc31, in terms of acceleration-displacement relationship, are shown together in Figs. 15 and 16, respectively. The same comparison is also made for the isolated floor system without edge plates (i.e., unidirectional seismic inputs and different load cases), for Load Cases 2 and 3 under shake table excitation input Acc31 (Fig. 17). From these figures, consistently, the floors subjected to greater gravity loads undergo lower peak accelerations. Because the bidirectional spring provides the same restoring force in this isolated floor system, when the mass supported by the floor is larger, the isolated period is longer, and the maximum acceleration response of the isolated floor is less.

Concentric versus Eccentric Load Cases

To investigate the difference in behavior between symmetric and eccentric load cases for this isolated floor system, the test results for 2Acc31 and 7Acc31 are compared in Fig. 18. It is observed that the behavior of the isolated floor system from each test agrees with each other well, which is consistent with the observation that the rotation effect of the isolated floor is not significant as mentioned before.

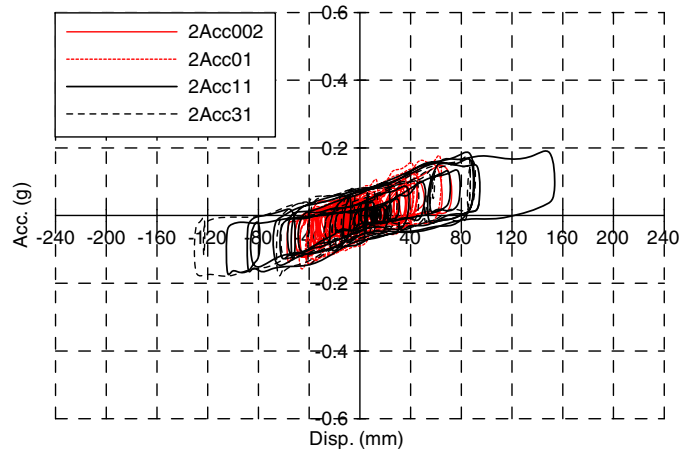

Fig. 13. Comparison of acceleration-displacement relationships under different inputs and load case 2

Effect of System Friction on Results

The presence of steel cover plates introduces friction between the plates and the surface of the isolated floor. To investigate the effect of this friction, the tests results for cases with and without these

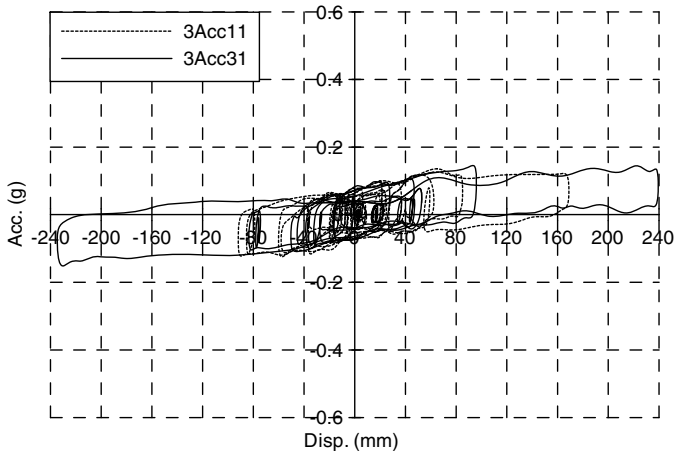

Fig. 14. Comparison of acceleration-displacement relationships under different inputs and load case 3

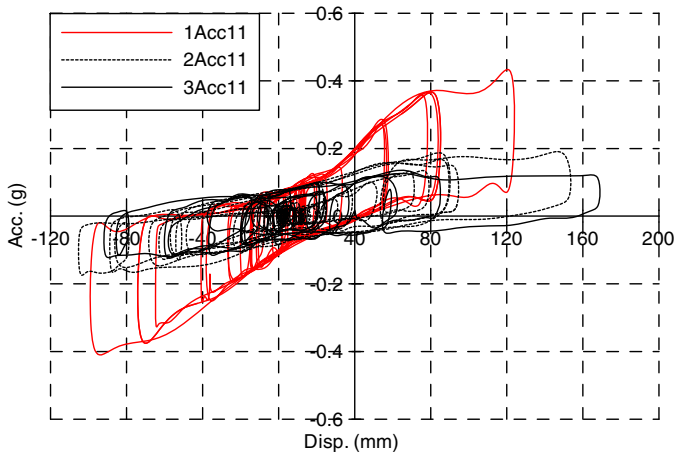

Fig. 15. Comparison of acceleration-displacement relationships under different symmetric load cases and same input of Acc11 (with edge plates)

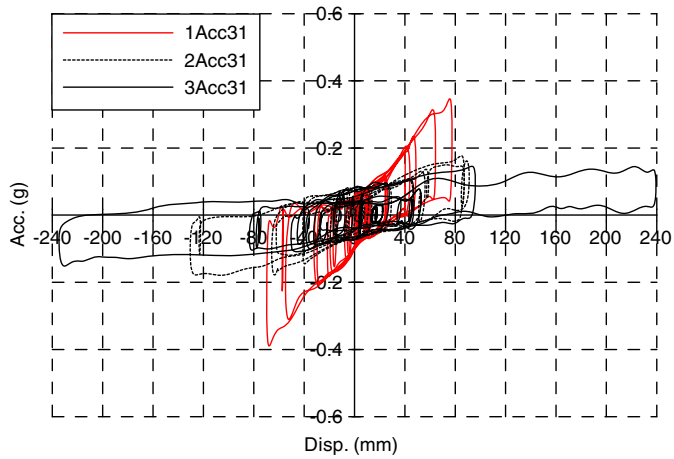

Fig. 16. Comparison of acceleration-displacement relationships under different symmetric load cases and same input of Acc31 (with edge plates)

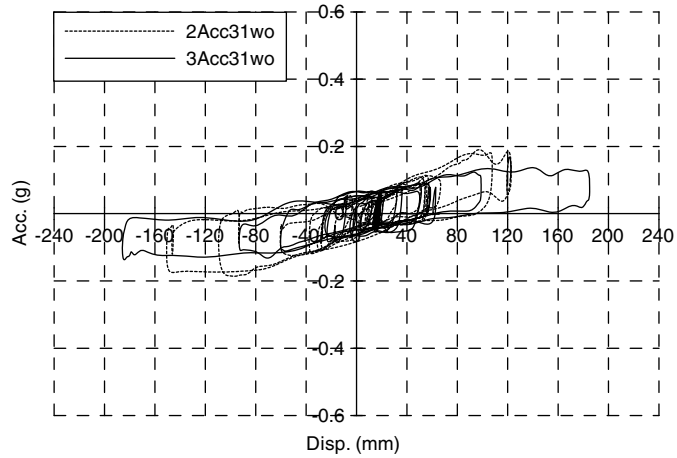

Fig. 17. Comparison of acceleration-displacement relationships under different symmetric load cases and same input of Acc31 (without edge plates)

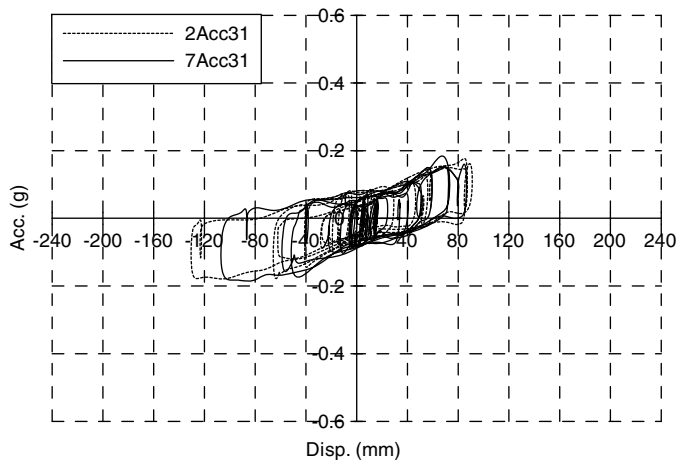

Fig. 18. Comparison of acceleration-displacement relationships between symmetric and eccentric load cases under input of Acc31

edge plates for Load Cases 2 and 3 under both unidirectional and bidirectional tests, in terms of acceleration-displacement relationships, are shown together for comparison in Figs. 19 and 20, respectively. Note that because the acceleration-displacement relationship of the isolated floor system in bidirectional tests is similar to that in unidirectional tests at relatively large displacement; the results for bidirectional tests were also included in this comparison. From these figures, note that there is no significant difference in the amplitude of the acceleration attained by the isolated floor under both unidirectional and bidirectional tests. This is reasonable because, although there is a friction force between the cover plates and the isolated floor surface, this force is almost negligible when compared with the total weight of the isolated floor system and imposed loads in Load Cases 2 and 3.

Fig. 21 compares the acceleration-displacement relationship for spring units from individual spring tests (Cui et al. 2012) and that of the overall isolated floor. The acceleration response from the spring units is almost zero when the displacement is near zero. However, it is not the case for the whole isolated floor system (without edge plates) where the acceleration response is approximately 0.035 g when the displacement is near zero. Also, the

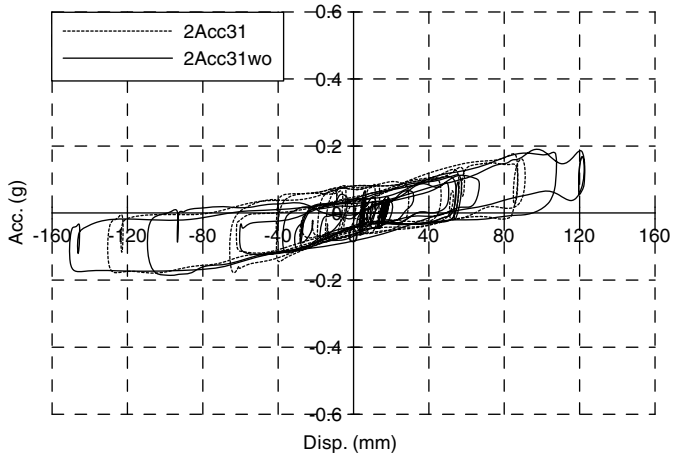

Fig. 19. Comparison of acceleration-displacement relationships between with and without cover plates under load case 2 when subjected to Acc31

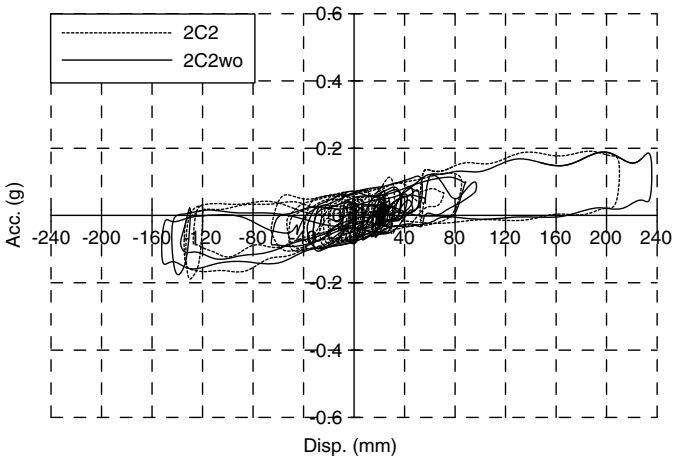

Fig. 20. Comparison of acceleration-displacement relationships in E-W direction between with and without cover plates under load case 2 when subjected to C2

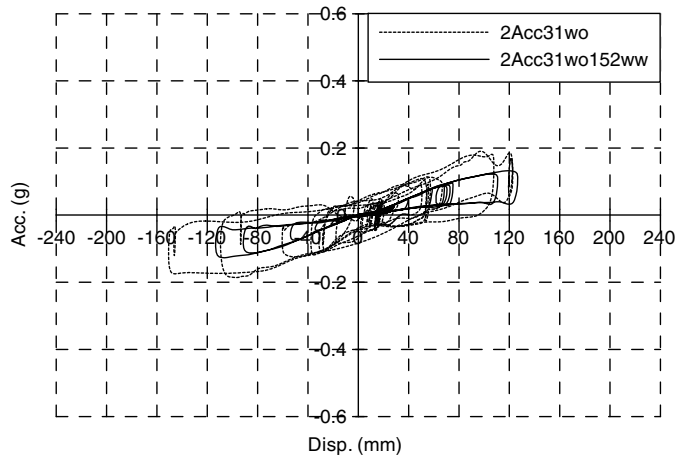

Fig. 21. Comparison of acceleration-displacement relationships between spring units and whole system under load case 2

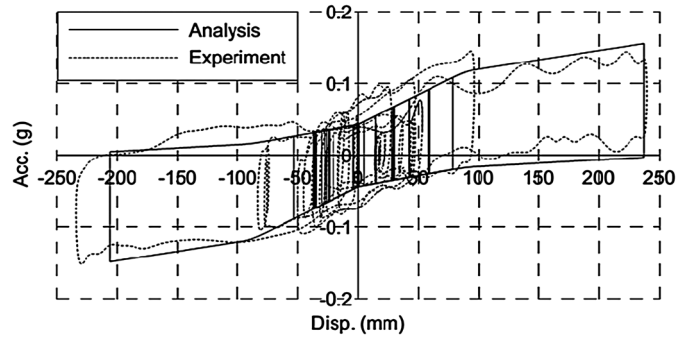

Fig. 22. Comparison between acceleration-displacement relationship results from analytical model and test for isolated floor system II using 2,627 N/m spring units, with edge plates, and under load case 3

acceleration-displacement loops for whole system tests are fatter than the corresponding ones for the spring units. The difference between these two groups of loops is approximately 0.035 g. This suggests that there exists a constant friction in the system, presumably between the casters and the concrete slab.

In addition, there is friction between the cover plates and the surface of the isolated floor. This friction force can be estimated from the weight of the cover plates and the friction coefficient between the steel plate and the floor. To accurately simulate the behavior of the complete system based on the behavior of the spring units, these extra friction forces shall be considered. Note that both frictions have the beneficial effect of providing initial rigidity to the floor isolation system.

To illustrate the need to include friction in models of the complete isolated floor system, an analytical model was built and implemented in *IDARC2D version 7.0*. This program was selected because it contained a hysteretic damper brace element that could be modified to be appropriate to simulate the behavior of the isolated floor system. First, the modified hysteretic element model incorporated in *IDARC2D* was set to replicate the behavior of the axial spring unit shown in Fig. 2 above. However, the zero-crossing of the hysteretic curves for the axial spring unit alone, compared with the experimental results presented in Figs. 5–10, shows that the analytical model must be expanded to account for the friction effect. The modified hysteretic damper brace element modeling the multidirectional spring units' behavior was therefore coupled with, in parallel, a friction damper brace element with almost rigid initial stiffness which considers both the friction effect from the casters and the friction effect from edge plates reported above.

Although details of analytical models, comparison with all experimental results, and sensitivity studies, will be the subject of a future paper and are beyond the scope of the current paper, for illustration purpose (in support of the observation that friction needs to be included in the analytical models), Fig. 22 shows a comparison of the results from the *IDARC2D* analyses (for the above described model) with the corresponding test results for the isolated floor system having 2,627 N/m (15 lb/in.) spring units, with edge plates, and under Load Case 3. Reasonable agreement is observed between the results from analysis and those from the corresponding test. The acceleration-displacement envelopes from the analysis are similar to those from the tests. Note that the friction effect (i.e., acceleration difference between the loading and unloading branches, including the restoring force of multidirectional spring units resulting from friction in the isolator bushings, and friction effects from casters and edge plates) is near that from the corresponding test, especially at relatively large displacement.

Importance of Quality Control

Although the previous sections illustrate that the isolated floor system worked well, it is important to emphasize here that before all these results were obtained, the isolated floor system was installed in a faulty manner that created unevenness on the floor surface. During the first tests, as the isolated floor moved, a tile of the walking surface protruded slightly above the adjacent ones and hit the edge of an edge plate during motion, and the isolated floor abruptly stopped moving when it happened, which caused high accelerations (with spikes of up to 1.5 g) on the isolated floor because of the sudden discontinuous jerky motion. In an actual implementation, it is recommend to implement a quality control program to prevent such a problem. Another (simpler) solution to this problem is to make the edge plates continuous over the seams of the tiles such that the problem will not rise.

Conclusions

Shake table test results show that the isolated floor system worked well in reducing the acceleration response on top of the isolated floor. The behavior of this isolated floor system for various nominal stiffness of the bidirectional spring units is stable when subjected to different seismic inputs for a given gravity load configuration and when subjected to repeated motions. Furthermore, in line with expectations, the peak acceleration of the isolated floor was found to decline when it supported greater gravity load owing to the fact that the same restoring force from the isolation system results in longer periods at higher loads.

It was found that at relatively large displacements (larger than 76 mm), the acceleration response of the isolated floor reaches a plateau. This is a function of the geometry of the system that results in a high initial stiffness and a much smaller secondary stiffness after 76 mm. The system's maximum acceleration response in bidirectional tests was found to be the same as in corresponding unidirectional tests as long as the displacement in both directions exceeded 76 mm, although their displacement response may be different.

The behavior of the entire isolated floor system was also compared with that of its bidirectional spring units, to generally identify how system-level nonlinear inelastic behavior differs from that of the springs alone. The observed difference in behavior was attributed to, first a constant friction value of 0.035 g attributed to the friction between the floor casters and the concrete base, and, second, to friction between the edge plates and the walking surface. These frictions, together with the model proposed in Cui et al. (2010) for bidirectional spring units, provide valuable data for better modeling the behavior of an isolated floor system.

Acknowledgments

This work was supported in whole by the Earthquake Engineering Research Centers Program of the National Science Foundation under Award No. ECC-9701471 to the Multidisciplinary Center for Earthquake Engineering Research. However, any opinions, findings, conclusions, and recommendations presented in this paper are those of the writers and do not necessarily reflect the views of the sponsors.

References

Arima, F., Tanaka, H., Takase, N., Egasira, H., and Nakamura, R. (1997). "Development of three-dimensional isolated floor systems." *Technical Rep. of Sumitomo Construction* (in Japanese).

Cui, S., Bruneau, M., and Constantinou, M. (2012). "Integrated design methodology for isolated floor systems in single-degree-of-freedom structural fuse systems." *Technical Rep. MCEER-12-0004*, MCEER, Univ. at Buffalo, Buffalo, NY, 478.

Cui, S., Bruneau, M., and Kasalanati, A. (2010). "Behavior of bidirectional spring unit in isolated floor systems." *J. Struct. Eng.*, 10.1061/(ASCE)ST.1943-541X.0000187, 944–952.

Demetriades, G. F., Constantinou, M. C., and Reinhorn, A. M. (1992). "Study of wire rope systems for seismic protection of equipment in buildings." *Rep. NCEER 92-12*, National Center for Earthquake Engineering Research, Univ. at Buffalo, Buffalo, NY.

Fathali, S., and Filiatrault, A. (2007). "Experimental seismic performance evaluation of isolation/restraint systems for mechanical equipment. Part I: Heavy equipment study." *Rep. No. MCEER-07-0007*, Multidisciplinary Center for Earthquake Engineering Research, Univ. at Buffalo, State Univ. of New York, Buffalo, NY.

IDARC2D version 7.0 [Computer software]. Engineering Seismology Laboratory, Univ. at Buffalo, Buffalo, NY.

Kaneko, M., Yasui, Y., and Okuda, Y. (1995). "Simultaneous horizontal and vertical vibration tests of three-dimensional floor isolation system." *AIJ J. Technol. Des.*, 1, 186–190.

Kasalanati, A., Reinhorn, A., Constantinou, M. C., and Sanders, D. (1997). "Experimental study of ball-in-cone isolation system." *Structures Congress XV*, ASCE, Reston, VA, 1191–1195.

Kemeny, Z. A., and Szidarovszky, F. (1995). "Seismic isolation bearings with nonlinear gravity restoring." *Rep. No. MCEER VF01127*, Multidisciplinary Center for Earthquake Engineering Research, Univ. at Buffalo, State Univ. of New York, Buffalo, NY.

Lambrou, V., and Constantinou, M. C. (1994). "Study of seismic isolation systems for computer floors." *Rep. NCEER 94-20*, National Center for Earthquake Engineering Research, Univ. at Buffalo, Buffalo, NY.

NEHRP. (2003). "NEHRP recommended provisions for seismic regulations for new buildings and other structures (FEMA 450)." Building Seismic Safety Council, National Institute of Buildings Sciences, Washington, DC.

SAP2000 [Computer software]. Computers and Structures Inc., Walnut Creek, CA.

Shi, Y., Becker, T. C., Furukawa, S., Sato, E., and Nakashima, M. (2014). "LQR control with frequency-dependent scheduled gain for a semi-active floor isolation system." *Earthquake Eng. Struct. Dyn.*, 43(9), 1265–1284.

TARSCTHS [Computer software]. Engineering Seismology Laboratory, Univ. at Buffalo, Buffalo, NY.

Vargas, R. E., and Bruneau, M. (2006a). "Analytical investigation of the structural fuse concept." *Rep. No. MCEER-06-0004*, Multidisciplinary Center for Earthquake Engineering Research, Univ. at Buffalo, State Univ. of New York, Buffalo, NY.

Vargas, R. E., and Bruneau, M. (2006b). "Experimental investigation of the structural fuse concept." *Rep. No. MCEER-06-0005*, Multidisciplinary Center for Earthquake Engineering Research, Univ. at Buffalo, State Univ. of New York, Buffalo, NY.

Wang, S.-J., et al. (2014). "Sloped multi-roller isolation devices for seismic protection of equipment and facilities." *Earthquake Eng. Struct. Dyn.*, 43(10), 1443–1461.